

# Multiscale Motion-Aware and Spatial-Temporal-Channel Contextual Coding Network for Learned Video Compression

Yiming Wang, *Student Member, IEEE*, Qian Huang, *Member, IEEE*, Bin Tang, *Member, IEEE*, Huashan Sun, and Xing Li

**Abstract**—Recently, learned video compression has achieved exciting performance. Following the traditional hybrid prediction coding framework, most learned methods generally adopt the motion estimation motion compensation (MEMC) method to remove inter-frame redundancy. However, inaccurate motion vector (MV) usually lead to the distortion of reconstructed frame. In addition, most approaches ignore the spatial and channel redundancy. To solve above problems, we propose a motion-aware and spatial-temporal-channel contextual coding based video compression network (MASTC-VC), which learns the latent representation and uses variational autoencoders (VAEs) to capture the characteristics of intra-frame pixels and inter-frame motion. Specifically, we design a multiscale motion-aware module (MS-MAM) to estimate spatial-temporal-channel consistent motion vector by utilizing the multiscale motion prediction information in a coarse-to-fine way. On the top of it, we further propose a spatial-temporal-channel contextual module (STCCM), which explores the correlation of latent representation to reduce the bit consumption from spatial, temporal and channel aspects respectively. Comprehensive experiments show that our proposed MASTC-VC is superior to previous state-of-the-art (SOTA) methods on three public benchmark datasets. More specifically, our method brings average 10.15% BD-rate savings against H.265/HEVC (HM-16.20) in PSNR metric and average 23.93% BD-rate savings against H.266/VVC (VTM-13.2) in MS-SSIM metric.

**Index Terms**—Learned video compression, motion estimation motion compensation, multiscale motion-aware module, spatial-temporal-channel contextual module, MASTC-VC.

## I. INTRODUCTION

WITH the rise of video applications such as YouTube and TikTok, short videos have become an extremely important media representation. People gradually have high demands on video resolution (eg., 1080p, 2K, 4K and even 8K videos) and smoothness, which are all dependent on video compression. Over the past twenty years, several recognized video compression standards including H.264/AVC [1], H.265/HEVC [2] and H.266/VVC [3] have been developed by the Joint Video Group (JVT). However, higher coding performance is often followed by an exponential increase of coding complexity and these hand-crafted modules cannot be jointly optimized in an end-to-end fashion.

Manuscript created October, 2023; (Corresponding author: Qian Huang)

Yiming Wang, Qian Huang, Bin Tang, Huashan Sun are with the school of computer and information, Hohai university, Nanjing, Jiangsu, 211100, China (email: isymwang@gmail.com, huangqian@hhu.edu.cn, cstb@hhu.edu.cn, sunhuashan@hhu.edu.cn).

Xing Li is with College of information Science and Technology, Nanjing Forestry University, Nanjing 210037, China (email: lixing@njfu.edu.cn)

In recent years, deep learning techniques are booming and developing rapidly. Ballé *et al.* [4] first introduce variational autoencoders to build an end-to-end learned image compression framework. Based on [4], many subsequent works [5]–[10] are proposed to make significant progress in improving rate distortion performance, even outperforming the best current hand-crafted video coding standard H.266/VVC [3] for intra-frame (I-frame) coding. The success of learned image compression has driven the rapid rise of learned video compression. Similar to classical hybrid coding frameworks, the learned video compression approaches replace traditional modules with deep neural networks for end-to-end rate distortion optimization (RDO). However, it is more challenging because both spatial and temporal redundancies need to be reduced.

From the coding perspective, current learned video compression methods [11]–[25] are roughly classified into two categories. **Motion prediction based method**: motion prediction utilizes the correlations between frames to get predicted information in pixel domain or feature domain. **Entropy coding based method**: advanced entropy model aims to capture spatial-temporal correlations to reduce redundancy. The above approaches correspond to two main aspects of optimization: 1) how to estimate accurate motion vector (MV) for prediction. 2) how to design efficient entropy coding models.

To estimate accurate motion vector, many methods have been proposed, such as pixel-level optical flow based methods [11], [13], [15], [16], space-space flow based method [14], multiple-frame method [12], feature-level prediction methods [17], [19] and convolutional LSTM (ConvLSTM) [26] based method [21]. However, optical flow based methods [11], [13], [15], [16] rely on dense flow for explicit learning, which makes it difficult to extract accurate motion information and may introduce extra artifacts in complicated non-rigid scenario. Faced with this situation, space-space flow based method [14] is proposed to extend the 2D flow field to the 3D space, leading to excessive spatial-temporal correlations. Multi-frame method [12] is also proposed to reduce this redundancy, but at the expense of complex motion prediction network. Feature-level prediction methods [17], [19] employ implicit learning, which mainly uses unsupervised learning to reconstruct the MV, avoiding the limitations introduced by optical flow. Nevertheless, it only uses the single-scale motion estimation strategy and ignores the spatial structure of motion field, resulting in less efficient motion representation. ConvLSTM based method

[21] takes spatial-temporal sequence prediction to model inter-frame motion and obtains progressive performance, however brings the burden of encoding side.

Meanwhile, several entropy coding models are designed to reduce redundancy. It can be divided into the residual coding based scheme [11]–[14], [16], [17], [21], [25] and conditional coding based scheme [18]–[20], [22], [24]. Among them, residual coding based scheme is suboptimal and uses only hand-crafted subtraction operations to remove redundancy. In contrast, conditional coding based scheme uses temporal context for entropy modeling and introduce hyper priors to reduce redundancy by transforming the marginal distribution model of coded symbols into a optimized joint model. However, current contextual models ignore the spatial context and channel context. This is because the hyper priors and contexts can be combined to predict the entropy model, which approximates the latent probability distribution more accurately.

In our work, we propose a motion-aware and spatial-temporal-channel contextual coding based video compression network (MASTC-VC). More specifically, we introduce a multiscale motion-aware module (MS-MAM) that introduces the coarse-to-fine strategy and utilizes the multiscale motion prediction information to extract spatial-temporal-channel consistent motion representations for more accurate MV. Furthermore, based on the contextual coding architecture, we design a spatial-temporal-channel contextual module (STCCM) to learn more precise spatial context, temporal context and channel context. Finally, we aggregate three contexts to enhance the prediction capabilities of the entropy model.

**Our contributions can be summarized as follows:**

- We propose a multiscale motion-aware module (MS-MAM), which explores the multiscale motion prediction information and performs coarse-to-fine strategy to estimate spatial-temporal-channel consistent MV.
- We propose a spatial-temporal-channel contextual module (STCCM) that aggregates spatial context, temporal context and channel context to reduce the bit-rate effectively.
- Extensive experimental results demonstrate that our proposed MASTC-VC outperforms the state-of-the-art (SOTA) methods on HEVC, UVG and MCL-JCV benchmark datasets.

## II. RELATED WORK

### A. Learned image compression

Compared with traditional image compression standards [27]–[29], learned image compression methods [4]–[10] have received more attention and reconstructed high-quality images while maintaining low bit rates. Mainly because these methods typically employ the auto-encoder framework that transforms input images into latent space to generate compact representations and design advanced entropy models to estimate their probability distributions.

In [4], Ballé *et al.* first propose a learned image compression network, which solves the backpropagation of quantization operations and takes a factorized entropy model to approximate the latent space distribution. Then, Ballé *et al.* [5] further introduce hyper priors that are seen as the side-information

to model spatial correlation, achieving results comparable to HEVC intra-frame coding [2]. Subsequent Minnen *et al.* [6] and Lee *et al.* [7] propose autoregressive models to construct a Gaussian mixture model (GMM), which outperforms the HEVC intra-frame coding. However, autoregressive model is performed sequentially for all spatial locations and is therefore quite slow. He *et al.* [9] propose two-step coding to solve the sequential coding problem without sacrificing performance. Cheng *et al.* [8] also propose a hybrid Gaussian model with results comparable to VVC intra-frame coding [2].

### B. Learned video compression

The progress of learned image compression has also driven the growth of learned video compression.

**Motion prediction based method.** The pioneering DVC [11] adopts a existing optical flow estimation network to perform temporal prediction. Afterwards, there have been some improvements in motion prediction coding. For example, Lin *et al.* [12] extend single reference frame to multiple frames to obtain more accurate MV. Agustsson *et al.* [14] propose a scale space flow estimation method, which use means of Gaussian blurring to transform 2D optical flow to 3D spaces. Hu *et al.* [15] propose resolution-adaptive flow coding method, where the optimal motion resolution is determined by the RDO strategy. Liu *et al.* [24] use motion representations of multi-scale flow field with joint spatio-temporal prior aggregation for motion coding. However, the optical flow estimation network is designed to generate accurate motion maps, which may not be optimal for video compression tasks. In addition, the above flow-based methods typically employ bilinear warping, which may introduces additional artifacts.

Subsequent FVC [17] is proposed to use deformable convolution (DCN) [30] to predict motion patterns in the feature space. Furthermore, Gao *et al.* [19] utilize the previous raw frame as an auxiliary reference information for motion prediction. Lin *et al.* [21] propose a ConvLSTM based method that explores more reference frames to model the motion representations. In general, accurate MV is crucial for motion prediction. For learned video compression methods, it is preferable for MV to be spatial-temporal-channel consistent.

**Entropy coding based method.** Another research direction is entropy coding. residual coding based schemes [11]–[14], [16], [17], [21], [25] use simple subtraction operations to remove redundancy between successive frames. Recently, conditional coding based scheme gradually attracts more and more attention, due to the fact that conditional coding consumes fewer bits. Li *et al.* [18] firstly move from residual coding to conditional coding, which learn temporal context and explore inter-frame correlation to remove redundancy automatically. Yang *et al.* [23] propose the recurrent probability entropy model which takes full advantage of temporal correlation to achieve efficient performance. Sheng *et al.* [31] design the feature propagation to learn temporal context more efficiently. The following work [20] further introduces conditional augmented normalizing flow to form a purified conditional coding structure. Jin *et al.* [22] also utilize multi-frequency components in temporal context for entropy coding.



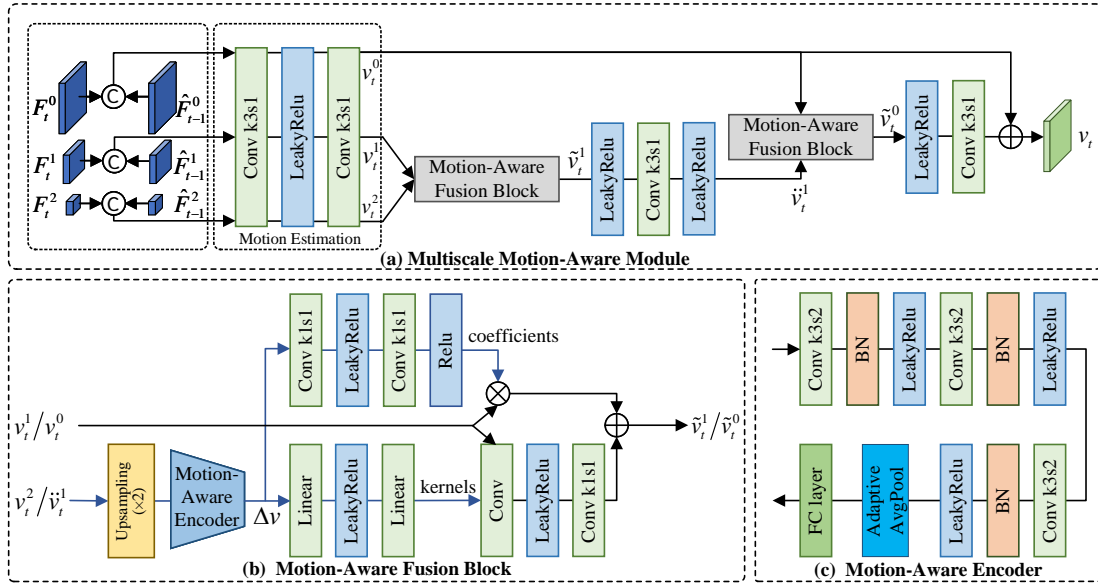


Fig. 3. The detailed network structures of (a) Multiscale Motion-Aware Module (MS-MAM), (b) Motion-Aware Fusion Block and (c) Motion-Aware Encoder.

**4) Motion Compensation:** We use DCN to warp the reconstructed MV  $\hat{v}_t$  with the reference frame feature  $\hat{F}_{t-1}^0$  to generate predicted feature  $\hat{F}_t$  in the motion compensation. (See III-C).

**5) Contextual Coding Module:** The current frame feature  $F_t^0$  and predicted feature  $\hat{F}_t$  are as conditions to extract spatial, temporal and channel contexts rather than simple subtraction operations to get contextual feature  $\hat{F}_t$ . Then it is refined to get reconstructed feature  $\hat{F}_t$ . We will introduce it in III-D.

**6) Frame Reconstruction:** As shown in Fig.2(b), the feature reconstruction with three residual blocks and a deconv layers will transform the final reconstructed feature  $\hat{F}_t$  into the pixel-level frame  $\hat{X}_t$ , which is stored in the reconstructed buffer (Rec.Buffer) for the following iterations.

### B. Multiscale Motion-Aware Module

Considering that inaccurate MV will affect the subsequent motion prediction and entropy coding, we propose a multiscale motion-aware module (MS-MAM) as illustrated in Fig.3, which performs motion estimation in a coarse-to-fine strategy. Specifically, we first concatenate multi-scale features  $F_t^i$ , and  $\hat{F}_{t-1}^i$ ,  $i = 0, 1, 2$  with the resolution of  $(H \times W, \frac{1}{2}H \times \frac{1}{2}W, \frac{1}{4}H \times \frac{1}{4}W)$  and fed them into the motion estimation module to generate initial temporal motion vectors  $(v_t^i, i = 0, 1, 2)$  with the size of  $(H \times W, \frac{1}{2}H \times \frac{1}{2}W, \frac{1}{4}H \times \frac{1}{4}W)$ .

$$v_t^i = \text{Conv}_{3 \times 3} \cdot \text{LeakyRelu} \cdot \text{Conv}_{3 \times 3} \cdot c(F_t^i, \hat{F}_{t-1}^i) \quad (2)$$

where  $c$  denotes concatenation along channel dimension,  $\text{Conv}_{3 \times 3}$  represents the convolution operations with  $3 \times 3$  kernel and  $\text{LeakyRelu}$  denotes the activation function.

Furthermore, our motion-aware fusion block uses the motion representation as conditions to predict the kernel of the convolution at the spatial level and also generates modulation coefficients at the channel level, respectively. In detail, initial small scale MV  $v_t^2$  is upsampled and then is encoded as motion-aware feature  $\Delta v$  by motion-aware encoder.

$$\Delta v = \text{MAE}(\text{upsampling}(v_t^2)) \quad (3)$$

where MAE represents the motion-aware encoder operations.

The architecture of motion-aware encoder is presented in Fig.3 (c) and it mainly consists of Convolution and BatchNorm layers. The final adaptive AvgPooling and Full Connected layers further integrate and utilize these feature representations to enable motion perception. On one hand, motion-aware feature  $\Delta v$  is fed into two linear layers to predict convolution kernels at the spatial level.

$$\text{kernels} = \text{Linear} \cdot \text{LeakyRelu} \cdot \text{Linear}(\Delta v) \quad (4)$$

where kernels denotes  $3 \times 3$  convolution kernels, Linear denotes a linear layer.

On the other hand, motion-aware feature  $\Delta v$  is fed into another two convolution layer and two activation function to generate modulation coefficients to perform channel feature adaptation.

$$\text{coefficients} = \text{Relu} \cdot \text{Conv}_{1 \times 1} \cdot \text{LeakyRelu} \cdot \text{Conv}_{1 \times 1}(\Delta v) \quad (5)$$

where  $\text{Conv}_{1 \times 1}$  represents  $1 \times 1$  convolution layer,  $\text{LeakRelu}$  and  $\text{Relu}$  denote the activation function.

Moreover, MV  $v_t^1$  is rescaled from different channels by  $\text{coefficients}$  to get channel components. MV  $v_t^1$  is processed with kernel-adaptive convolution and  $1 \times 1$  convolution layer to get spatial components. Finally, channel component features and spatial component features are summed to obtain the coarse MV  $\tilde{v}_t^1$  with  $\frac{1}{2}H \times \frac{1}{2}W$  size.

$$\tilde{v}_t^1 = \text{coefficients} \otimes v_t^1 + \text{Conv}_{1 \times 1} \cdot \text{LeakyRelu} \cdot \text{Conv}_{\text{kernels}}(v_t^1) \quad (6)$$

where  $\otimes$  denotes multiplication,  $\text{Conv}_{\text{kernels}}$  represents the convolution layer with the predicted kernels.

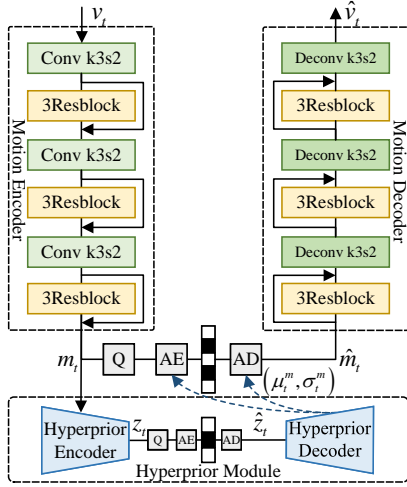


Fig. 4. Illustration of the motion encoder-decoder framework. Q represents quantization. AE and AD denote arithmetic encoder and arithmetic decoder.  $\mu_t^m$  and  $\sigma_t^m$  are the mean and variance value from hyperprior module.

Then, MV  $\tilde{v}_t^1$  is passed to a series of operations including LeakyRelu activation function and convolution layer to generate the coarse MV  $\tilde{v}_t^1$ .

$$\tilde{v}_t^1 = \text{LeakyRelu} \cdot \text{Conv}_{3 \times 3} \cdot \text{LeakyRelu}(\tilde{v}_t^1) \quad (7)$$

Besides, coarse MV  $\tilde{v}_t^1$  with  $\frac{1}{2}H \times \frac{1}{2}W$  size and  $v_t^0$  with  $H \times W$  resolution is fed into the motion-aware fusion block to generate MV  $\tilde{v}_t^0$  with  $H \times W$  size.

$$\tilde{v}_t^0 = \text{Motion-Aware-Fusion-Block}(\tilde{v}_t^1, v_t^0) \quad (8)$$

Finally,  $\tilde{v}_t^0$  is fed into a convolution layer and  $v_t^0$  is summed to obtain a refined spatial-temporal-channel consistent MV  $v_t$  with  $H \times W$  size at the time step  $t$ .

$$v_t = v_t^0 + \text{Conv}_{3 \times 3} \cdot \text{LeakyRelu}(\tilde{v}_t^0) \quad (9)$$

### C. Motion Encoder-Decoder and Motion Compensation

After MV  $v_t$  is generated, it will be passed to our proposed variational auto-encoder style networks and then bitstream is transferred to the decoder side for motion compensation. The Motion Encoder-Decoder module is depicted in Fig.4. This module contains motion encoder and motion decoder that both are made up of a set of residual blocks [32]. The architecture of residual blocks is shown in Fig.2(c). MV  $v_t$  is encoded as feature representation  $m_t$  by motion encoder and  $m_t$  is quantized as  $\hat{m}_t$  which will be used for entropy coding. Furthermore, we use hyperprior module [5] to estimate the mean  $\mu_t^m$  and variance  $\sigma_t^m$  value of Gaussian scale mixture.

$$\begin{cases} z_t = \text{Hyperprior\_Encoder}(m_t) \\ \mu_t^m, \sigma_t^m = \text{Hyperprior\_Decoder}(\hat{z}_t) \end{cases} \quad (10)$$

where  $z_t$  is the hyperprior feature representation and  $\hat{z}_t$  denotes quantized hyperprior feature representation.

We build entropy model  $p_{\hat{m}}$  and fit the marginal probability distribution  $q_{\hat{m}}$ . According to the Shannon entropy, the encoding lower bound for modeling the feature representation using the estimated entropy model  $p_{\hat{m}}$  is:

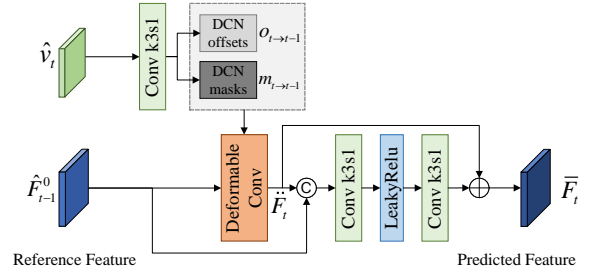


Fig. 5. Network architecture of Motion Compensation using deformable convolution.

$$\begin{aligned} R(\hat{m}) &= \mathbb{E}_{\hat{m} \sim q_{\hat{m}}} [-\log_2 p_{\hat{m}}(\hat{m})] \\ &= -\sum_t q(\hat{m}_t) \log_2 p_{\hat{m}_t}(\hat{m}_t) \end{aligned} \quad (11)$$

where  $q_{\hat{m}}$  denotes real probability distribution,  $p_{\hat{m}}$  is formulated as Gaussian scale mixture parameterized by  $(\mu_t^m, \sigma_t^m)$ . The above cross entropy can be more accurately optimized when the probability distribution predicted by the entropy coding model  $p_{\hat{m}}$  is the same as the actual probability distribution  $q_{\hat{m}}$ . Total number of bits consumed by motion is the sum of  $R(\hat{m}_t)$  and  $R(\hat{z}_t)$  at the time step  $t$ . Subsequently quantized features  $\hat{m}_t$  is used to reconstruct the MV  $\hat{v}_t$  in the Motion Decoder.

The network architecture of motion compensation is shown in Fig.5. Specifically, We utilize the reconstructed MV to compute the DCN offsets  $o_{t \rightarrow t-1}$  and modulation mask  $m_{t \rightarrow t-1}$ .

$$o_{t \rightarrow t-1}, m_{t \rightarrow t-1} = \text{Conv}_{3 \times 3}(\hat{v}_t) \quad (12)$$

where  $o_{t \rightarrow t-1}$  represents DCN offsets,  $m_{t \rightarrow t-1}$  represents DCN masks. DCN is then used to warp reconstructed MV  $\hat{v}_t$  with the reference frame feature  $\hat{F}_{t-1}^0$  with the resolution of  $H \times W$  to produce intermediate feature  $\ddot{F}_t$ .

$$\ddot{F}_t = \text{DCN}(o_{t \rightarrow t-1}, m_{t \rightarrow t-1}, \hat{F}_{t-1}^0) \quad (13)$$

Finally, we concatenate intermediate feature  $\ddot{F}_t$  and reference feature  $\hat{F}_{t-1}^0$  to get predicted feature  $\bar{F}_t$ .

$$\bar{F}_t = \ddot{F}_t + \text{Conv}_{3 \times 3} \cdot \text{LeakyRelu} \cdot \text{Conv}_{3 \times 3}(c(\ddot{F}_t, \hat{F}_{t-1}^0)) \quad (14)$$

### D. Contextual Coding Module

Previous video compression methods mainly reduce redundancy from temporal dimension, which have emerged with residual coding schemes and conditional coding based schemes. According to the information theory, the entropy of residual coding is equal to or larger than the contextual coding scheme. Therefore, we use conditional coding based scheme. Our contextual coding module mainly contains contextual encoder-decoder, refinement and STCCM, which is described in Fig.6.

The current feature  $F_t^0$  and predicted feature  $\bar{F}_t$  are concatenated to fed into the contextual encoder module to get contextual feature representation  $c_t$ .

$$c_t = \text{Contextual\_Encoder}(c(F_t^0, \bar{F}_t)) \quad (15)$$

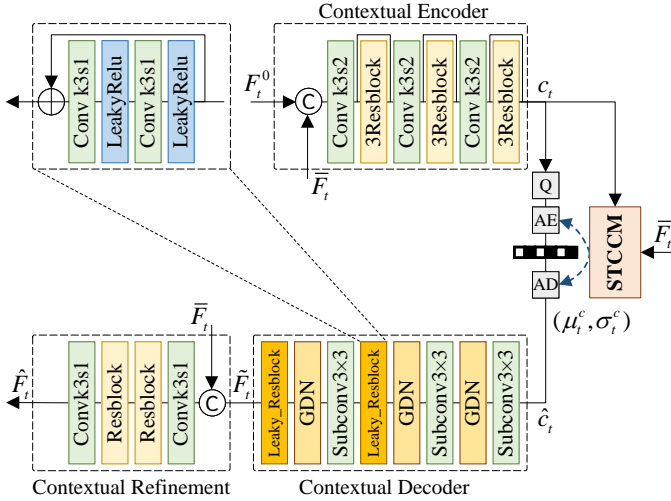


Fig. 6. Illustration of contextual coding module. STCCM is used to estimate the probability distribution.

We visualize the entropy of contextual feature representation  $c_t$ . From Fig.8, We find that there exists information aggregation in the contextual coding scheme for learned video compression and it is obvious to see that the entropy of previous four groups decreases gradually, however this phenomenon does not apply to the last four groups. This is because the previous four groups features are produced from the current uncompressed features encoded by contextual encoder, whereas the last four groups features are derived from the predicted features. The current features are transformed from the pixel space to the latent space, just like the transformation of traditional video compression into the frequency domain, where the information is gathered in the initial channel. Besides, predicted features are generative and go through the motion encoder-decoder module, so we finally split the channel dimensions into 4 chunks with  $\{16, 16, 32, 64\}$  channels respectively. Subsequent ablation experiments will further verify the effectiveness of our proposed STCCM.

Fig.7 illustrates our proposed spatial-temporal-channel contextual module (STCCM). We apply the hyperprior module and temporal context model to extract hyperprior  $\hat{s}_t$  and temporal prior  $t_t$ . Then  $\hat{s}_t$  and  $t_t$  are fused to utilize temporal correlation and generate temporal context  $c_t^{temporal}$ . Furthermore, we introduce spatial and channel contextual encoder to explore spatial-channel correlation for the channel context  $c_t^{channel}$  and spatial context  $c_t^{spatial}$ , respectively. To improve computational efficiency, we adopt the checkboard method [9] for spatial correlation.

$$\begin{cases} \hat{s}_t = \text{Hyperprior\_Module}(c_t) \\ t_t = \text{Temporal\_Contextual\_Encoder}(\bar{F}_t) \\ c_t^{temporal} = \text{Prior\_Fusion}(\hat{s}_t, t_t) \\ c_t^{channel} = \text{Channel\_Contextual\_Encoder}(\hat{c}_t^{(k)}) \\ c_t^{spatial} = \text{Spatial\_Contextual\_Encoder}(\hat{c}_t^{(k)}) \end{cases} \quad (16)$$

Three contexts information  $c_t^{temporal}$ ,  $c_t^{channel}$  and  $c_t^{spatial}$  are concatenated and fed into context aggregation to predict entropy parameter  $(\mu_t^c, \sigma_t^c)$  of every chunk for the following decoding  $\hat{c}_t^{(k)}$ . Decoded  $k$ -dimensional feature channel  $\hat{c}_t^{(k)}$

will be used as conditions to extract the following channel context  $c_t^{channel}$  and spatial context  $c_t^{spatial}$  with temporal context  $c_t^{temporal}$ , till reconstruct the entire contextual feature representation  $\hat{c}_t$ .

Moreover, we build contextual entropy model  $p_{\hat{c}}$  to fit probability distribution  $q_{\hat{c}}$ . According to the Shannon entropy, the encoding lower bound for modelling the feature representation using the estimated entropy model  $p_{\hat{c}}$  is:

$$R(\hat{c}) = \mathbb{E}_{\hat{c} \sim q_{\hat{c}}} [-\log_2 p_{\hat{c}}(\hat{c})] = - \sum_t q(\hat{c}_t) \log_2 p_{\hat{c}_t}(\hat{c}_t) \quad (17)$$

Therefore, the total number of bits consumed by context is the sum of  $R(\hat{c}_t)$  and  $R(\hat{s}_t)$  at the time step  $t$ .

Reconstructed context  $\hat{c}_t$  is decoded as contextual feature  $\bar{F}_t$ . Then,  $\bar{F}_t$  and  $\bar{F}_t$  are concatenated to be refined as reconstructed current feature  $\hat{F}_t$ . Finally,  $\hat{F}_t$  is transformed into reconstructed frame  $\hat{X}_t$ .

### E. Loss Function

Our proposed scheme aims to minimize the coding bitrate cost while reducing the distortion between current frame and reconstructed frame. We use the following rate-distortion (RD) loss function for training:

$$\begin{aligned} L_t &= \lambda D + R \\ &= \frac{1}{T} \sum_t \left\{ \lambda d(X_t, \hat{X}_t) + R(\hat{m}_t) + R(\hat{z}_t) + R(\hat{c}_t) + R(\hat{s}_t) \right\} \end{aligned} \quad (18)$$

where  $d(\cdot)$  denotes the mean-square-error (MSE) / 1-MS-SSIM [33] for PSNR/MS-SSIM metric.  $R(\hat{m}_t)$  denotes the encoding quantized motion vector feature representation and  $R(\hat{z}_t)$  denotes the associated hyper prior of MV.  $R(\hat{c}_t)$  denotes the encoding quantized contextual feature representation and  $R(\hat{s}_t)$  denotes the associated hyper prior of contextual feature.  $\lambda$  denotes the Langrange factor.  $T$  is the time interval.

## IV. EXPERIMENTS

### A. Datasets and Experimental Setup

**Datasets:** Following previous works, we employ Vimeo-90K [34] as a training dataset, which contains 89800 video clips and each clips have 7 successive frames with the resolution of  $448 \times 256$ . During the training phase, the videos are cropped with  $256 \times 256 \times 3$  size. Furthermore, we use the HEVC datasets, UVG datasets [35] and MCL-JCV [36] datasets to measure video coding performance. Specifically, the HEVC datasets contains the video sequences with various resolutions of  $1920 \times 1080$  (Class B),  $832 \times 480$  (Class C),  $416 \times 240$  (Class D) and  $1280 \times 720$  (Class E). The Ultra Video Group (UVG) contains 7 high frame rate  $1920 \times 1080$  video sequences. MCL-JCV dataset contains 30  $1920 \times 1080$  videos collected from YouTube.

**Evaluation Methodologies:** We adopt the bit per pixel (Bpp) to measure the bit consumption and use PSNR/MS-SSIM metrics to evaluate the distortion between the original frame and reconstructed frame. Besides, we set the group of picture

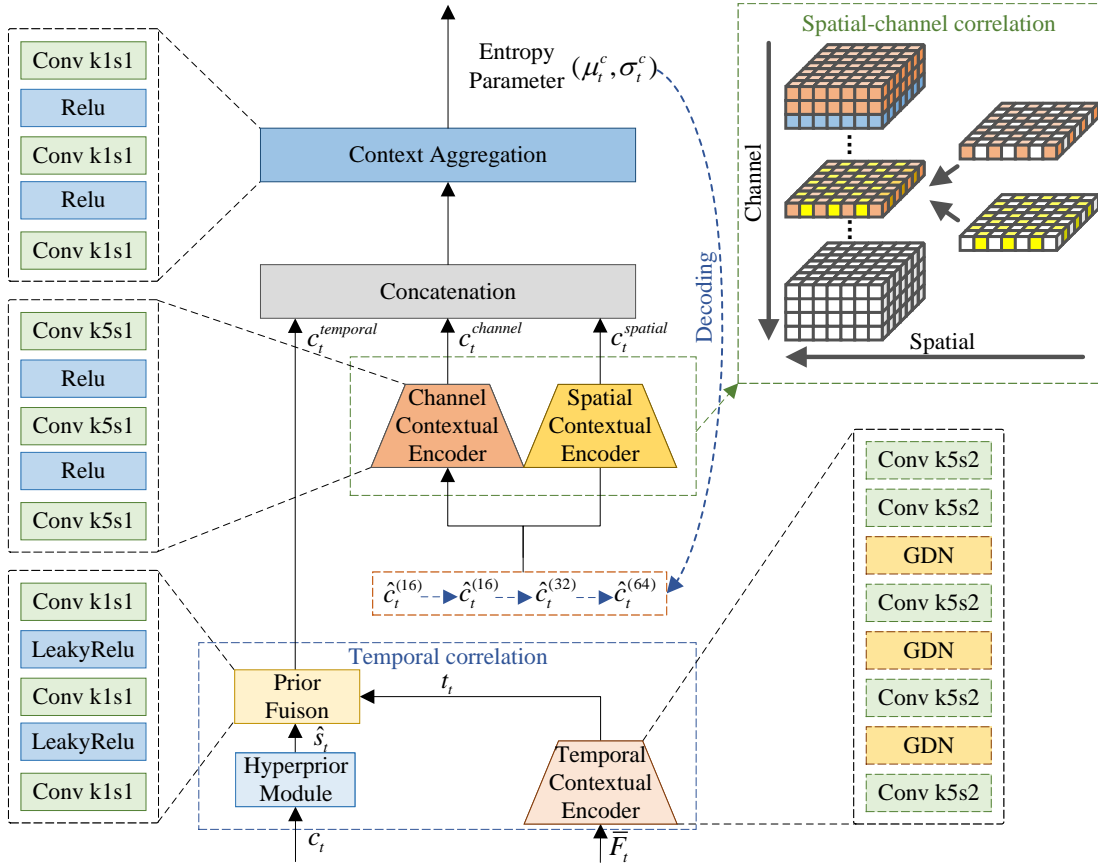


Fig. 7. Diagram of proposed spatial-temporal-channel contextual module (STCCM). Temporal, spatial and channel contexts are aggregated to estimate the entropy parameter.

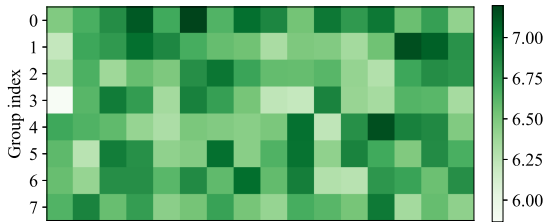


Fig. 8. Entropy of each feature channel. The results are evaluated on the HEVC Class B. Darker colors represent greater entropy.

(GOP) size as 10 for HEVC datasets and 12 for other datasets as previous works settings. In addition, we set x265(verslow) as the anchor used to report BD-rates.

**Implementation Details:** We take a two-stage strategy to train our model. At the first stage, we set  $T$  as 1 in Eq.(18) and utilize successive frame information including I-frame and P-frame for 2,000K steps with the learning-rate of  $5e-5$  to achieve a baseline model. At the second stage, we take a widely-used training strategy [37], which sets  $T$  as 6 in Eq.(18) and extends the length of training video sequences to 7 frames for another 500K steps with the learning-rate of  $5e-6$  to avoid error propagation. When using MS-SSIM metric, we further fine-tune the model from stage 2 for 100K steps by using 1- MS-SSIM as distortion loss. Our proposed MASTC-VC is built by Pytorch 1.13 with CUDA 12.1. We set the batch size as 4 at the first stage and 2 at the remaining stage. We take 5 days to construct the entire experiments on the machine with

a single NVIDIA 4090 GPU (24GB memory).

### B. Experimental Results

**Baseling Methods Settings:** To evaluate the coding performance of our proposed MASTC-VC, we use traditional coding standards H.265/HEVC [2], H.266/VVC [3] as well as the SOTA learned video compression methods including FVC [17], DCVC [18], SPME(FVC\*) [19], SPME(DCVC) [19], CANF-VC [20], DMVC [21] and TCVC [22]. Following previous work, we use the *Cheng2020\_Anchor(MSE/MS-SSIM)* [8] provided by CompressAI [40] for I frame coding. The other prediction (P) frames are coded sequentially by their individual network.

For the current popular coding standards H.265/HEVC [2], we use the industrial software x265 (verslow) and official reference software HM-16.20 (LDP) [38] as:

- x265 (verslow)
 

```
ffmpeg -pixfmt yuv420p -s WxH
-r FR -i Input.yuv -v frames N
-c:v libx265 -preset verslow
-tune zerolatency -x265 -params
"crf=QP:keyint=GOP:verbose=1"
output.mkv
```
- HM-16.20 (LDP)
 

```
TAppEncoder -c encoder_lowdelay_P_main.cfg
-i input.yuv -DecodingRefreshType=2
-f N -q QP -fr FR -wdt W -hgt H
-IntraPeriod=12 -o output.yuv
```

TABLE I  
BD-RATE(%) SAVING COMPARISON BETWEEN EXISTING BASELINE METHODS AND THE ANCHOR IS x265(VERYSLOW) IN PSNR METRICS. THE BEST PERFORMANCE OF LEARNED METHODS IS MARKED IN BOLD>.

Datasets	Traditional Methods					Learned Methods					Ours
	HM-16.20 [38] (LDP, 4refs)	VTM-13.2 [39] (LDP, 8refs)	FVC [17] (CVPR'21)	DCVC [18] (NIPS'21)	SPME(FVC*) [19] (ACMMM'22)	SPME(DCVC) [19] (ACMMM'22)	CANF-VC [20] (ECCV'22)	DMVC [21] (TCSVT'23)	TCVC [22] (TIP'23)		
HEVC ClassB	-30.53	-53.23	-15.83	-32.04	-23.25	-35.56	-33.15	-32.12	-40.52	<b>-45.90</b>	
HEVC ClassC	-18.59	-42.39	-4.55	-6.29	-0.41	-10.72	-13.24	-13.77	-15.58	<b>-15.87</b>	
HEVC ClassD	-17.50	-40.34	-1.51	-11.74	-6.22	-15.48	-15.68	-18.51	-24.08	<b>-24.91</b>	
HEVC ClassE	-46.91	-69.03	-35.16	-28.79	-24.12	-32.90	-28.27	-41.48	-44.14	<b>-48.05</b>	
UVG	-30.26	-53.17	-32.06	-34.66	-26.03	-48.75	-39.84	-36.68	-38.58	<b>-54.54</b>	
MCL-JCV	-17.57	-40.44	-17.44	-20.32	1.25	-30.30	-22.17	-14.81	-21.07	<b>-32.96</b>	
AVG	-26.89	-49.77	-17.76	-22.31	-13.13	-28.95	-25.39	-26.23	-30.66	<b>-37.04</b>	

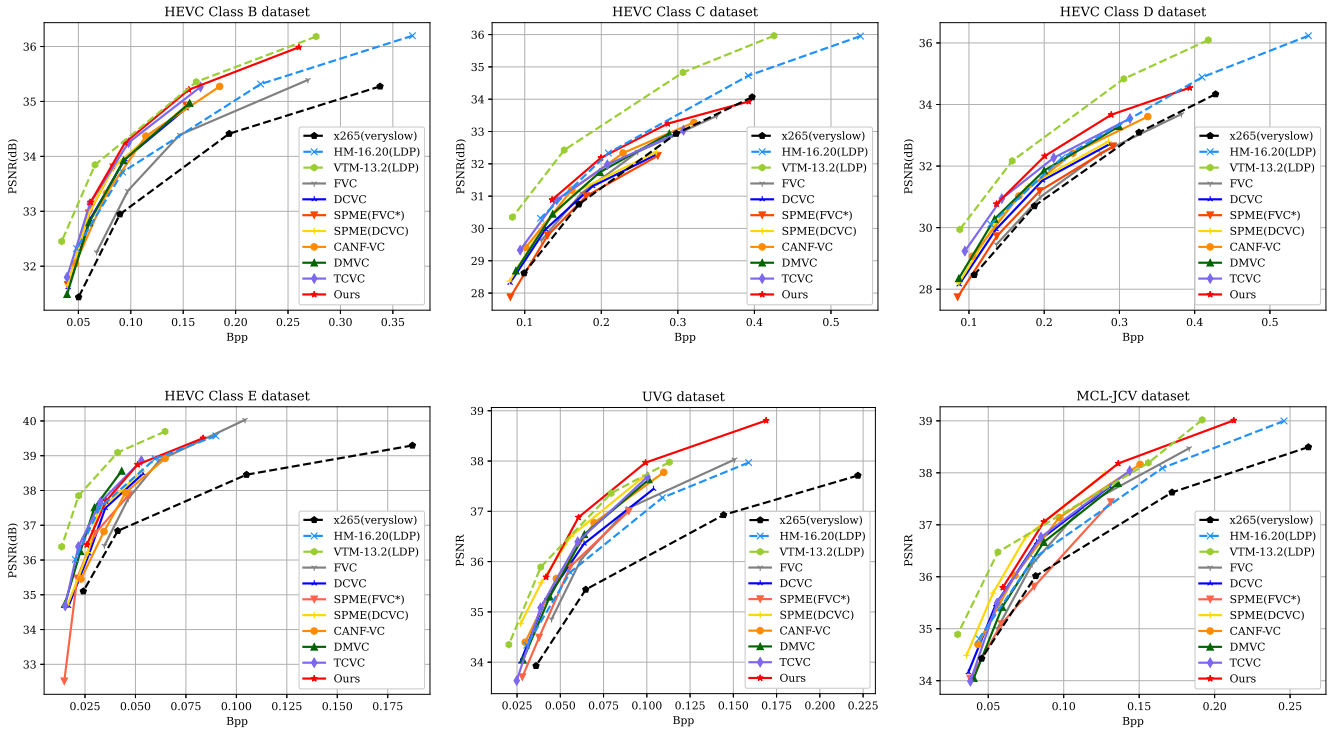


Fig. 9. Rate-distortion performance evaluation of our proposed method on the HEVC, UVG and MCL-JCV datasets in PSNR metrics.

For the latest coding standards H.266/VVC [3], we use the official reference software VTM-13.2 (LDP) [39] as:

- VTM-13.2 (LDP)

```
EncoderApp -c encoder_lowdelay_P_vtm.cfg
-i input.yuv -DecodingRefreshType=2
-f N -q QP -fr FR -wdt W -hgt H
-IntraPeriod=16 -o output.yuv
```

In these settings,  $W$ ,  $H$ ,  $FR$ ,  $N$ ,  $GOP$  represent width, height, frame rate, encoded frame numbers and the  $GOP$  size, respectively. The quantization parameter (QP) is set as  $\{21, 23, 27, 31\}$ . Furthermore, we also discuss the influence of different  $GOP$  size in subsequent ablation study.

**Coding Performance in PSNR metric:** Table I shows the Bjøntegaard Delta Bit-Rate (BDBR) [41] performance for PSNR metric using the anchor as x265 (veryslow). The lower BD-rate value, the more bit cost reduced, indicating better coding performance. As shown in the Table I, our

proposed method achieves 37.04% BD-rate saving on average. On one hand, traditional methods HM-16.20 [38] and VTM-13.2 [39] bring 26.89% and 49.77% coding gain on average. On the other hand, learned methods FVC [17], DCVC [18], SPME(FVC\*) [19], SPME(DCVC) [19], CANF-VC [20], DMVC [21] and TCVC [22] save 17.76%, 22.31%, 13.13%, 28.95%, 25.39%, 26.23% and 30.66% BD-rate on average, respectively. It is obvious to see that our scheme is superior to FVC, DCVC, SPME(FVC\*), SPME(DCVC), CANF-VC, DMVC and TCVC on all benchmark datasets, which proves the strong generalization ability of our proposed MASTC-VC. Moreover, we also beat popular HM-16.20 by average 10.15% coding gain. More importantly, we outperform the latest VTM-13.2 on UVG dataset. The corresponding results can also be seen from the RD curves in Fig.9. However, our scheme cannot catch up with the VTM-13.2 in general, although we achieve the SOTA coding performance in the learned methods.

TABLE II

BD-RATE(%) SAVING COMPARISON BETWEEN EXISTING BASELINE METHODS AND THE ANCHOR IS x265(VERSLow) IN MS-SSIM METRICS. THE BEST PERFORMANCE OF LEARNED METHODS IS MARKED IN BOLD.

Datasets	Traditional Methods		Learned Methods								Ours
	HM-16.20 [38] [38] (LDP, 4refs)	VTM-13.2 [39] [39] (LDP, 8refs)	FVC [17] (CVPR'21)	DCVC [18] (NIPS'21)	SPME(FVC*) [19] (ACMMM'22)	SPME(DCVC) [19] (ACMMM'22)	CANF-VC [20] (ECCV'22)	DMVC [21] (TCSVT'23)	TCVC [22] (TIP'23)		
HEVC ClassB	-14.21	-41.24	-47.42	-44.08	-40.44	-47.60	-48.02	-51.12	-58.03	<b>-76.06</b>	
HEVC ClassC	-7.93	-34.18	-39.11	-36.30	-34.49	-39.00	-44.76	-43.52	-45.60	<b>-55.86</b>	
HEVC ClassD	-5.86	-31.82	-46.22	-45.46	-44.34	-48.75	-50.64	-54.57	-51.56	<b>-58.43</b>	
HEVC ClassE	-27.87	-57.98	-59.80	-35.50	-34.35	-44.64	-44.65	-58.93	-54.68	<b>-72.99</b>	
UVG	-14.10	-41.80	-42.46	-42.58	-32.91	-49.26	-48.81	-49.27	-48.28	<b>-58.19</b>	
MCL-JCV	-2.40	-32.36	-44.54	-41.38	-32.22	-45.03	-42.86	-45.56	-46.98	<b>-61.45</b>	
AVG	-12.06	-39.90	-46.59	-40.88	-36.46	-45.71	-46.62	-50.50	-50.86	<b>-63.83</b>	

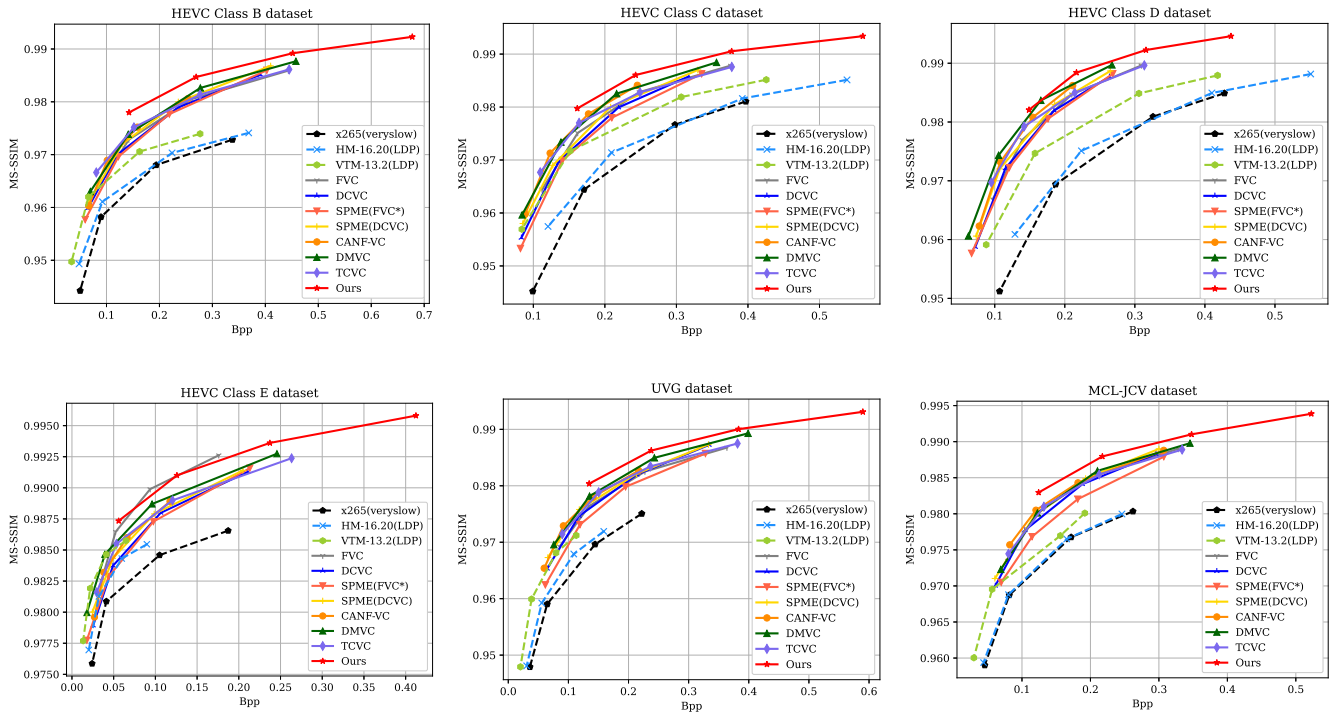


Fig. 10. Rate-distortion performance evaluation of our proposed method on the HEVC, UVG and MCL-JCV datasets in MS-SSIM metrics.

**Coding Performance in MS-SSIM metric:** Table II shows the BDBR performance for MS-SSIM metric using the anchor as x265 (veryslow). From TableII, our method achieves 63.83% BD-rate reduction on average. Meanwhile, the traditional methods (HM-16.20, VTM-13.2) bring 12.06% and 39.9% BD-rate increase on average, respectively. Also, the learned methods (FVC [17], DCVC [18], SPME(FVC\*) [19], SPME(DCVC) [19], CANF-VC [20], DMVC [21] and TCVC [22]) get 46.59%, 40.88%, 36.46%, 45.71%, 46.62%, 50.50% and 50.86% BD-rate saving on average, respectively. It can be found that the rate-distortion performance of the learned methods is better than the traditional methods, which indicates the potential of data-driven video coding methods in MS-SSIM metric. Furthermore, Our proposed MASTC-VC surpasses the listed learned method [17]–[22] and traditional methods (HM-16.20 [38] , VTM-13.2 [39] ) by a larger margin on all test datasets, especially on high-resolution (1080p) video datasets. It is important to highlight that our method outperforms the

VTM-13.2 by 23.93% in MS-SSIM metrics. The corresponding results can also be seen from the RD curves in Fig.10.

**Visual Comparison:** To further evaluate the strength of our proposed method (MASTC-VC), we also provide the visualization of HM-16.20 [38] , VTM-13.2 [39] , DCVC [18], SPME(FVC\*) [19], DMVC [21] and our MASTC-VC in Fig.11. It can be obviously seen that our MASTC-VC model can obtain better reconstructed frame quality with less bit consumption than other methods. Specifically, the QP for HM-16.20 and VTM-13.2 is set as 21. We set the  $\lambda$  as 2048 for the learned video compression. It is worth noting that our method can retain high-fidelity texture.

### C. Ablation Study

**Effectiveness of the Proposed MS-MAM and STCCM:** In this work, we pay more attention on motion prediction and contextual coding modules. Hence, we propose the multi-scale motion-aware module (MS-MAM) and spatial-temporal-

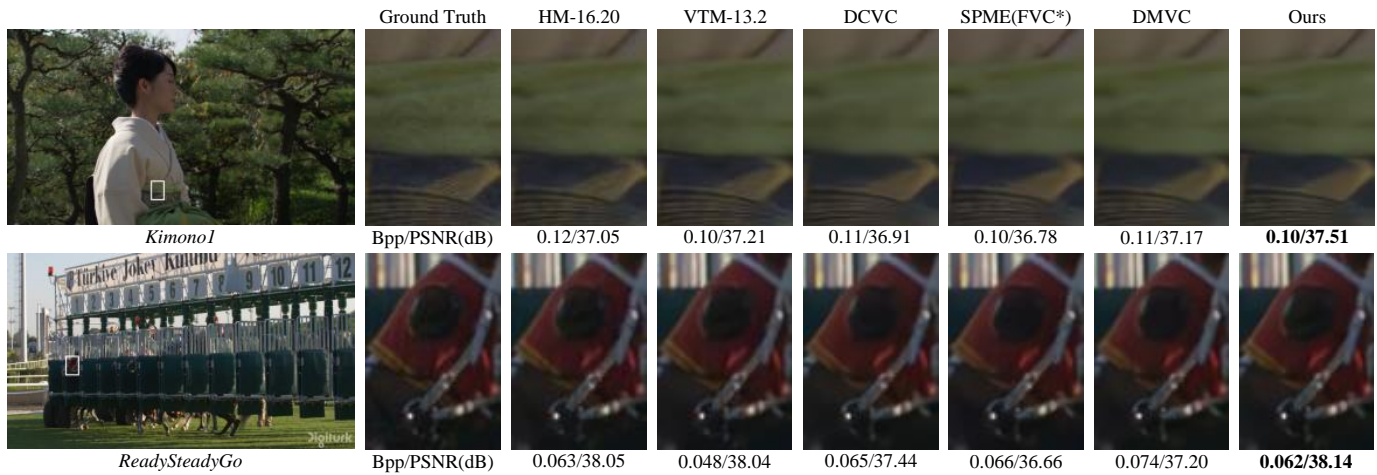


Fig. 11. The reconstructed frame from HM-16.20, VTM-13.2, DCVC, SPME(FVC\*), DMVC and our proposed method.

TABLE III  
EFFECTIVENESS OF THE PROPOSED DIFFERENT MODULES OF OUR SCHEME.

MS-MAM	STCCM	B	C	D	E	UVG	MCL-JCV
✓	✓	0.0	0.0	0.0	0.0	0.0	0.0
✓	✗	2.9	8.2	5.5	1.1	6.0	2.6
✗	✓	3.7	2.6	3.3	9.1	9.7	3.3
✗	✗	8.3	18.9	14.0	11.6	14.2	6.6

channel contextual module (STCCM). To validate the contributions of proposed MS-MAM and STCCM, we perform an ablation study as shown in Table III, where the baseline is our full model (MS-MAM + STCCM). From the Table III, we can find that the MS-MAM and STCCM both can improve the compression ratio. As shown in Fig.12, we also take the *RaceHorses\_416×240\_30* sequence as an example to visualize inter-frame motion information, reconstructed error and reconstructed frame quality. It can be observed that our proposed MASTC-VC and "w/ MS-MAM w/o STCCM" model can generate additional spatial hierarchy in Fig.12 (a), which illustrates the effectiveness of MS-MAM. Moreover, the proposed MASTC-VC and "w/o MS-MAM w/ STCCM" model reconstruct higher quality frames with less bit consumption in Fig.12 (b) and (c), indicating that the effectiveness of STCCM.

TABLE IV  
INFLUENCE OF THREE DIFFERENT CONTEXTS OF OUR STCCM.

	B	C	D	E	UVG	MCL-JCV
w/o spatial context	3.6	3.5	2.2	1.9	10.2	6.0
w/o channel context	5.7	4.9	3.7	2.3	11.5	9.0
w/o temporal context	12.3	17.2	11.5	9.8	15.4	9.8

**Influence of Three Different Contexts:** Furthermore, we aggregate the three contexts to improve the coding performance in spatial-temporal-channel contextual module. We execute ablation studies to explore the influence of three different contexts. Table IV compares the performance influence of spatial, temporal and channel contexts. The baseline is our full

model. It is obvious to see that the three different contexts improve the rate-distortion performance to varying degrees. Among them, the improvement of temporal context is larger than other contexts, mainly owing to the strong correlation between successive frames.

TABLE V  
INFLUENCE OF THE CHANNEL GROUPING OF OUR STCCM

	B	C	D	E	UVG	MCL-JCV
(16,16,16,16,16,16,16)	3.1	1.7	2.9	6.2	14.4	3.6
(16,16,16,16,64)	3.9	2.5	2.1	5.9	13.5	5.7
(16,48,64)	4.3	2.3	1.7	3.3	11.6	6.8

**Influence of the Channel Grouping:** To study the influence of the channel grouping of our STCCM, we change the number of channel grouping. The baseline is our final grouping solution. As depicted in Table V, the BD-rate reduction of our final grouping solution is the highest. Our scheme initially uses fewer channels to assign finer granularity to the beginning chunks and gradually allocates coarser granularity by using more channels, which better fits the latent sapce distribution.

TABLE VI  
THE CODING PERFORMANCE OF DIFFERENT GOP SIZE. THE ANCHOR IS THE GOP10.

	B	C	D	E
GOP 4	26.6	23.4	31.1	59.3
GOP 8	4.3	2.9	4.4	8.3
GOP 12	-2.0	-1.3	-2.5	-5.2
GOP 16	-3.9	-2.5	-4.9	-9.7
GOP 32	-3.3	0.73	-5.4	-7.5

**Different GOP Size:** The GOP (group of pictures) is used to alleviate the error propagation. However, larger GOP sizes will cause reconstructed frame quality decreases and smaller GOP sizes will increase bits cost. We make the experiment to discuss the influence of different GOP size. Table VI shows the RD performance of different GOP size of our proposed method. As we can see from this table, the GOP choice is often a trade-off. The GOP 16 is the optimal for HEVC Class B, C and E. Yet, GOP 32 is optimal for HEVC Class D.

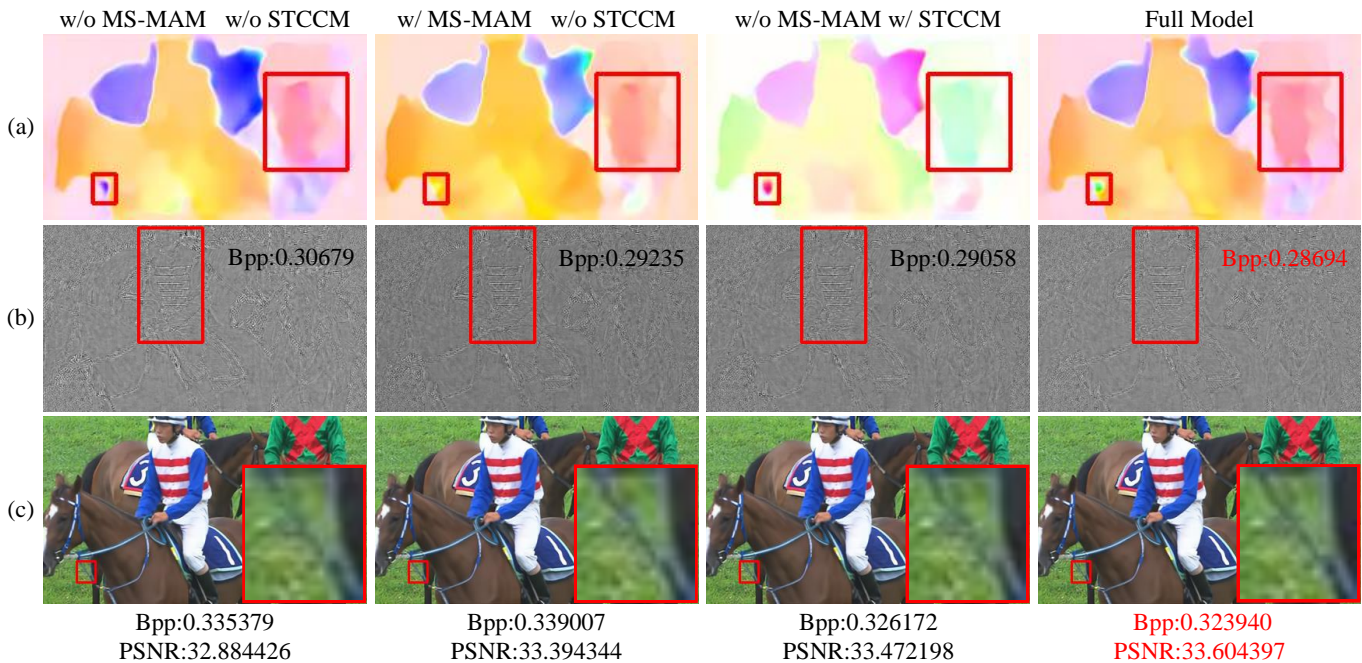


Fig. 12. Visualizing the (a) temporal motion, (b) reconstructed error and (c) reconstructed frame quality.

TABLE VII

THE RATE-DISTORTION PERFORMANCE OF DIFFERENT INTRA CODING METHOD IN PSNR METRIC. THE ANCHOR IS CHENG2020\_ANCHOR

	B	C	D	E	UVG	MCL-JCV
HM-16.20 intra coding [38]	9.7	-0.1	9.1	10.5	17.5	19.3
VTM-13.2 intra coding [39]	-2.4	-8.6	0.5	-10.6	4.1	9.9
bmshj2018_hyperprior [5]	23.3	3.0	11.5	37.1	18.3	13.8
mbt2018 [6]	14.8	-2.5	4.6	14.2	10.2	6.8

#### D. Model Analysis

**Influence of Intra Coding Method:** It is well known that I-frames also have an influence on the final encoding performance. Therefore, we also discuss the impact of different intra-frame coding methods on the overall coding performance. We select the learned image compression methods bmshj2018\_hyperprior [5], mbt\_2018 [6], cheng2020\_anchor [8] as well as the traditional methods HM-16.20 intra coding [38], VTM-13.2 intra coding [39]. Detailed experimental results are shown in Table VII, where cheng2020\_anchor is used as an anchor. It can be observed that we can get better RD performance when more efficient intra-frame coding methods are applied.

**Computational Complexity:** We also have measured the computational complexity of our proposed method on NVIDIA RTX 4090 and our model has 19.87M float parameters. Furthermore, we select the traditional codec (x265, HM-16.20 [38], VTM-13.2 [39]) and learned methods including FVC [17], DCVC [18], SPME(FVC\*) [19], CANF-VC [20], DMVC [21] and TCVC [22] to encode the 1080p videos. Average encoding and decoding speed is listed in Table VIII.

It is obvious to see that FVC [17] is faster than our method (MASTC-VC), which is owing to the fact that it is based on simple residual coding structures without complex

TABLE VIII

AVERAGE ENCODING/DECODING SPEED (FRAMES PER SECOND) AND MODEL PARAMETERS ON 1080P VIDEOS

Method	Params(M)	Enc Speed	Dec Speed
x265 (veryslow)	-	0.28	19.23
HM-16.20 (LDP) [38]	-	0.03	10.2
VTM-13.2 (LDP) [39]	-	0.001	1.2
FVC [17]	20.07	4.08	6.67
DCVC [18]	7.94	0.082	0.028
SPME(FVC*) [19]	17.75	2.57	-
CANF-VC [20]	31	0.625	0.95
DMVC [21]	23.96	1.83	-
TCVC [22]	28.8	0.072	0.013
Ours	19.87	3.24	5.32

contextual entropy coding networks. However our proposed method slightly slows the speed of encoding/decoding and we have achieved higher encoding performance than other learned methods. In the future, we will design efficient architectures to reduce coding complexity.

#### V. CONCLUSION AND DISCUSSION

In this paper, we propose a learned video compression (MASTC-VC) via motion-aware and spatial-temporal-channel contextual coding module. In particular, the MS-MAM is proposed to utilize the multiscale motion prediction information to estimate spatial-temporal-channel consistent MV in a coarse-to-fine fashion. Furthermore, the STCCM is proposed to exploit the correlation of latent representation to reduce the bit consumption from spatial, temporal and channel respectively. Lastly, quantitative and qualitative experimental results have demonstrated that our proposed method is superior to previous state-of-the-art (SOTA) methods in terms of both PSNR and MS-SSIM metrics.

## REFERENCES

- [1] T. Wiegand, G. Sullivan, G. Bjontegaard, and A. Luthra, "Overview of the h.264/avc video coding standard," *IEEE Transactions on Circuits and Systems for Video Technology*, vol. 13, no. 7, pp. 560–576, 2003.
- [2] G. J. Sullivan, J.-R. Ohm, W.-J. Han, and T. Wiegand, "Overview of the high efficiency video coding (hevc) standard," *IEEE Transactions on Circuits and Systems for Video Technology*, vol. 22, no. 12, pp. 1649–1668, 2012.
- [3] B. Bross, Y.-K. Wang, Y. Ye, S. Liu, J. Chen, G. J. Sullivan, and J.-R. Ohm, "Overview of the versatile video coding (vvc) standard and its applications," *IEEE Transactions on Circuits and Systems for Video Technology*, vol. 31, no. 10, pp. 3736–3764, 2021.
- [4] J. Ballé, V. Laparra, and E. P. Simoncelli, "End-to-end optimized image compression," in *5th International Conference on Learning Representations, ICLR, 2017*.
- [5] J. Ballé, D. Minnen, S. Singh, S. J. Hwang, and N. Johnston, "Variational image compression with a scale hyperprior," in *6th International Conference on Learning Representations, ICLR, 2018*.
- [6] D. Minnen, J. Ballé, and G. Toderici, "Joint autoregressive and hierarchical priors for learned image compression," in *Proc. Adv. Neural Inf. Process. Syst. (NIPS)*, pp. 10794–10803, 2018.
- [7] J. Lee, S. Cho, and S. Beack, "Context-adaptive entropy model for end-to-end optimized image compression," in *7th International Conference on Learning Representations, ICLR, 2019*.
- [8] Z. Cheng, H. Sun, M. Takeuchi, and J. Katto, "Learned image compression with discretized gaussian mixture likelihoods and attention modules," in *2020 IEEE/CVF Conference on Computer Vision and Pattern Recognition (CVPR)*, pp. 7936–7945, 2020.
- [9] D. He, Y. Zheng, B. Sun, Y. Wang, and H. Qin, "Checkerboard context model for efficient learned image compression," in *2021 IEEE/CVF Conference on Computer Vision and Pattern Recognition (CVPR)*, pp. 14766–14775, 2021.
- [10] D. He, Z. Yang, W. Peng, R. Ma, H. Qin, and Y. Wang, "Elic: Efficient learned image compression with unevenly grouped space-channel contextual adaptive coding," in *2022 IEEE/CVF Conference on Computer Vision and Pattern Recognition (CVPR)*, pp. 5708–5717, 2022.
- [11] G. Lu, W. Ouyang, D. Xu, X. Zhang, C. Cai, and Z. Gao, "Dvc: An end-to-end deep video compression framework," in *2019 IEEE/CVF Conference on Computer Vision and Pattern Recognition (CVPR)*, pp. 10998–11007, 2019.
- [12] J. Lin, D. Liu, H. Li, and F. Wu, "M-lvc: Multiple frames prediction for learned video compression," in *2020 IEEE/CVF Conference on Computer Vision and Pattern Recognition (CVPR)*, pp. 3543–3551, 2020.
- [13] G. Lu, C. Cai, X. Zhang, L. Chen, W. Ouyang, D. Xu, and Z. Gao, "Content adaptive and error propagation aware deep video compression," in *Proc. Eur. Conf. Comput. Vis. ECCV*, vol. 12347, pp. 456–472, 2020.
- [14] E. Agustsson, D. Minnen, N. Johnston, J. Ballé, S. J. Hwang, and G. Toderici, "Scale-space flow for end-to-end optimized video compression," in *2020 IEEE/CVF Conference on Computer Vision and Pattern Recognition (CVPR)*, pp. 8500–8509, 2020.
- [15] Z. Hu, Z. Chen, D. Xu, G. Lu, W. Ouyang, and S. Gu, "Improving deep video compression by resolution-adaptive flow coding," in *Proc. Eur. Conf. Comput. Vis. ECCV*, vol. 12347, pp. 193–209, 2020.
- [16] G. Lu, X. Zhang, W. Ouyang, L. Chen, Z. Gao, and D. Xu, "An end-to-end learning framework for video compression," *IEEE Transactions on Pattern Analysis and Machine Intelligence*, vol. 43, no. 10, pp. 3292–3308, 2021.
- [17] Z. Hu, G. Lu, and D. Xu, "Fvc: A new framework towards deep video compression in feature space," in *2021 IEEE/CVF Conference on Computer Vision and Pattern Recognition (CVPR)*, pp. 1502–1511, 2021.
- [18] J. Li, B. Li, and Y. Lu, "Deep contextual video compression," in *Proc. Adv. Neural Inf. Process. Syst. (NIPS)*, pp. 18114–18125, 2021.
- [19] H. Gao, J. Cui, M. Ye, S. Li, Y. Zhao, and X. Zhu, "Structure-preserving motion estimation for learned video compression," in *Proceedings of the 30th ACM International Conference on Multimedia, MM '22*, p. 3055–3063, 2022.
- [20] Y. Ho, C. Chang, P. Chen, A. Gnutti, and W. Peng, "CANF-VC: conditional augmented normalizing flows for video compression," in *Proc. Eur. Conf. Comput. Vis. ECCV*, vol. 13676, pp. 207–223, 2022.
- [21] K. Lin, C. Jia, X. Zhang, S. Wang, S. Ma, and W. Gao, "Dmvc: Decomposed motion modeling for learned video compression," *IEEE Transactions on Circuits and Systems for Video Technology*, vol. 33, no. 7, pp. 3502–3515, 2023.
- [22] D. Jin, J. Lei, B. Peng, Z. Pan, L. Li, and N. Ling, "Learned video compression with efficient temporal context learning," *IEEE Transactions on Image Processing*, vol. 32, pp. 3188–3198, 2023.
- [23] R. Yang, F. Mentzer, L. Van Gool, and R. Timofte, "Learning for video compression with recurrent auto-encoder and recurrent probability model," *IEEE Journal of Selected Topics in Signal Processing*, vol. 15, no. 2, pp. 388–401, 2021.
- [24] H. Liu, M. Lu, Z. Ma, F. Wang, Z. Xie, X. Cao, and Y. Wang, "Neural video coding using multiscale motion compensation and spatiotemporal context model," *IEEE Transactions on Circuits and Systems for Video Technology*, vol. 31, no. 8, pp. 3182–3196, 2021.
- [25] H. Liu, M. Lu, Z. Chen, X. Cao, Z. Ma, and Y. Wang, "End-to-end neural video coding using a compound spatiotemporal representation," *IEEE Transactions on Circuits and Systems for Video Technology*, vol. 32, no. 8, pp. 5650–5662, 2022.
- [26] X. SHI, Z. Chen, H. Wang, D.-Y. Yeung, W.-k. Wong, and W.-c. WOO, "Convolutional lstm network: A machine learning approach for precipitation nowcasting," in *Proc. Adv. Neural Inf. Process. Syst. (NIPS)*, vol. 28, Curran Associates, Inc., 2015.
- [27] G. Wallace, "The jpeg still picture compression standard," *IEEE Transactions on Consumer Electronics*, vol. 38, no. 1, pp. xviii–xxxiv, 1992.
- [28] A. Skodras, C. A. Christopoulos, and T. Ebrahimi, "The JPEG 2000 still image compression standard," *IEEE Signal Process. Mag.*, vol. 18, no. 5, pp. 36–58, 2001.
- [29] F. Bellard, "Bpg image format." <http://bellard.org/bpg/>. Accessed: 2018-10-30. 1, 2.
- [30] J. Dai, H. Qi, Y. Xiong, Y. Li, G. Zhang, H. Hu, and Y. Wei, "Deformable convolutional networks," in *2017 IEEE International Conference on Computer Vision (ICCV)*, pp. 764–773, 2017.
- [31] X. Sheng, J. Li, B. Li, L. Li, D. Liu, and Y. Lu, "Temporal context mining for learned video compression," *IEEE Transactions on Multimedia*, pp. 1–12, 2022.
- [32] K. He, X. Zhang, S. Ren, and J. Sun, "Deep residual learning for image recognition," in *2016 IEEE Conference on Computer Vision and Pattern Recognition (CVPR)*, pp. 770–778, 2016.
- [33] Z. Wang, E. Simoncelli, and A. Bovik, "Multiscale structural similarity for image quality assessment," in *The Thirty-Seventh Asilomar Conference on Signals, Systems & Computers*, vol. 2, pp. 1398–1402 Vol.2, 2003.
- [34] T. Xue, B. Chen, J. Wu, D. Wei, and W. T. Freeman, "Video enhancement with task-oriented flow," *International Journal of Computer Vision (IJCV)*, vol. 127, no. 8, pp. 1106–1125, 2019.
- [35] A. Mercat, M. Viitanen, and J. Vanne, "UVG dataset: 50/120fps 4k sequences for video codec analysis and development," in *Proceedings of the 11th ACM Multimedia Systems Conference (MMSys)*, pp. 297–302, 2020.
- [36] H. Wang, W. Gan, S. Hu, J. Y. Lin, L. Jin, L. Song, P. Wang, I. Katsavounidis, A. Aaron, and C.-C. J. Kuo, "Mcl-jvc: A jnd-based h.264/avc video quality assessment dataset," in *2016 IEEE International Conference on Image Processing (ICIP)*, pp. 1509–1513, 2016.
- [37] G. Lu, C. Cai, X. Zhang, L. Chen, W. Ouyang, D. Xu, and Z. Gao, "Content adaptive and error propagation aware deep video compression," in *Proc. Eur. Conf. Comput. Vis. ECCV*, pp. 456–472, 2020.
- [38] HM-16.20. <https://vcgit.hhi.fraunhofer.de/jvet/HM/>. Accessed: 2022-07-05.
- [39] VTM-13.2. [https://vcgit.hhi.fraunhofer.de/jvet/VVCSoftware\\_VTM/](https://vcgit.hhi.fraunhofer.de/jvet/VVCSoftware_VTM/). Accessed: 2022-03-02.
- [40] J. Bégin, F. Racapé, S. Feltman, and A. Pushparaja, "Compressai: a pytorch library and evaluation platform for end-to-end compression research," *arXiv preprint arXiv:2011.03029*, 2020.
- [41] G. Bjontegaard, "Calculation of average psnr differences between rd-curves," *VCEG-M33*, 2001.